



**You have downloaded a document from
RE-BUŚ
repository of the University of Silesia in Katowice**

Title: Role of the molybdenum addition on the mechanical properties and structure of the NiCoMnIn alloys

Author: Krystian Prusik, Edyta Matyja, M. Wąsik, Maciej Zubko

Citation style: Prusik Krystian, Matyja Edyta, Wąsik M., Zubko Maciej. (2019). Role of the molybdenum addition on the mechanical properties and structure of the NiCoMnIn alloys. "Archives of Metallurgy and Materials" (2019, iss. 2, s. 733-738), DOI: 10.24425/amm.2019.127606



Uznanie autorstwa - Użycie niekomercyjne - Licencja ta pozwala na kopiowanie, zmienianie, remiksowanie, rozprowadzanie, przedstawienie i wykonywanie utworu jedynie w celach niekomercyjnych. Warunek ten nie obejmuje jednak utworów zależnych (mogą zostać objęte inną licencją).



UNIwersYTET ŚLĄSKI
W KATOWICACH



Biblioteka
Uniwersytetu Śląskiego



Ministerstwo Nauki
i Szkolnictwa Wyższego

K. PRUSIK^{*,**}, E. MATYJA^{*,**}, M. WĄSIK^{*}, M. ZUBKO^{*,**}

ROLE OF THE MOLYBDENUM ADDITION ON THE MECHANICAL PROPERTIES AND STRUCTURE OF THE NiCoMnIn ALLOYS

In this paper, the influence of Mo addition on the structure and mechanical properties of the NiCoMnIn alloys have been studied. Series of polycrystalline NiCoMnIn alloys containing from 0 to 5 mas.% of Mo were produced by the arc melting technique. For the alloys containing Mo, two-phase microstructure was observed. Mo-rich precipitates were distributed randomly in the matrix. The relative volume fraction of the precipitates depends on the Mo content. The numbers of the Mo rich precipitates increases with the Mo contents. The structures of the phases were determined by the TEM. The mechanical properties of the alloys are strongly affected by Mo addition contents. Brittleness of the alloys increases with the Mo contents.

Keywords: MSMA, martensite, structure, NiCoMnIn, additions, shape memory

1. Introduction

NiCoMnIn alloys as magnetic shape memory alloys (MSMA) exhibit reversible martensitic transformation which may be driven either by temperature, external strain or magnetic field resulting in macroscopic shape change [1,2]. Large recoverable strain and high-frequency response make this material promising magnetic actuators [3]. Despite of many advantages, NiCoMnIn alloys are very brittle. There are many strategies to improve the ductility of ordered intermetallic crystal structures including controlling of phase stability, eliminating environmental embrittlement, promoting transformation induced plasticity, structure, and chemistry grain-boundary engineering. One of the ways is to control or introduce the appropriate texture to the materials [4,5]. But the most useful method is microstructural optimization which may be realized by thermal treatment and/or chemical composition selection (e.g. by appropriate elements additions) [6-9].

Usually, in the case of Ni-Mn based MSMA, a third or/and fourth element is added to improve the magnetic properties or shift the martensitic transformation temperatures. Very often it can also modify the structure. In the Ni_{49.9}Mn_{37.1}Sn_{13.0} substitution of Ni by 1 at% Co increases the martensitic temperatures so the magnetocaloric effect as well [10]. A Co doping of Ni-Mn-Sn increases the Curie temperature of austenite [11]. The substitution by niobium in Ni₄₅Co₅Mn₄₀Sn₁₀ shifts the transformation temperatures downwards accompanied by a reduction of the magnetocaloric effect [12].

The role of Mo addition on MSMA is not clear but the matrix composition plays a very important role. On one hand, Mo can play positive role e.g. in the high performance cast iron (HPCI) with improved mechanical properties using in the application of automobile components [13]. X. Ding et.al observed almost a 20% increase of the ultimate tensile stress (UTS) when the 0.55wt.% of molybdenum was added. Also for TiC/Al composites doped by 1-5wt% of Mo the 14% the UTS increase was observed [14]. Y. Chen et al. [15] studied the Mo addition role on the Ti-Ni-Nb shape memory alloys. They stated that for Ni_{45.0-x}Ti_{46.0}Nb_{9.0}Mo_x (x = 0, 0.5, 1.0, 1.5 at.%) yield strength and rupture strength are enhanced with increasing Mo content, while the elongation is reduced slightly and remains still at a high level. On the other hand, Mo is one of the main element and is widely added to biomedical Ni-free Ti-based Shape Memory Alloys such as Ti-Nb-Mo [16], Ti-Mo-Sn [17], Ti-Mo-Ga [18].

Until now the role of Mo in the context of the MSMA has not been investigated yet. So the main aim of the present study is to determine the influence of Mo addition on the structure and mechanical properties of the NiCoMnIn MSMA alloys.

2. Experimental (materials and methods)

Series of 10 grams of polycrystalline magnetic shape memory alloys (MSMA) specimens (buttons) of the given nominal chemical composition Ni_{45.5}Co_{4.5}Mn_{36.6}In_{13.4} (at.%) with the 0-5wt.% (0, 0.5, 1, 2, 5 wt.%) of molybdenum addition was

* UNIVERSITY OF SILESIA, INSTITUTE OF MATERIALS SCIENCE, 75 PUŁKU PIECHOTY 1A STR., 41-500 CHORZÓW, POLAND

** SILESIA CENTRE FOR EDUCATION AND INTERDISCIPLINARY RESEARCH, 12 BANKOWA STR., 40-007 KATOWICE, POLAND

*** UNIVERSITY OF HRADEC KRÁLOVÉ, DEPARTMENT OF PHYSICS, HRADEC KRÁLOVÉ, CZECH REPUBLIC

Corresponding author: krystian.prusik@us.edu.pl

prepared by the arc melting technique. In order to homogenize each button were remelted 5 to 8 times, subsequently thermally treated at 1173 for 24 h in vacuum quartz capsules. Specimens with the increasing Mo contents (0-5wt.%) were denoted as Mo0, Mo0.5 Mo1, Mo2, and Mo5 respectively. The microstructure of the studied alloys was observed by the JEOL JSM-6480 scanning electron microscope (SEM). The structure was examined by the high-resolution JEOL JEM3010 transmission electron microscope (TEM) and by electron backscatter diffraction (EBSD) technique (HKL system equipped with NordlysII camera). Thin foil for TEM was prepared by Gatan PIPS ion miller. The chemical composition of the alloys was measured by IXRF Energy Dispersive X-Ray Spectroscopy (EDXS) detector using standard calibration method. The mechanical properties of the samples were studied by compression test on the testing machine setup. The specimens for the test have a form of a rectangular prism of the size $3 \times 3 \times 4$ mm.

3. Results and discussions

The SEM microstructure of the $\text{Ni}_{45.5}\text{Co}_{4.5}\text{Mn}_{36.6}\text{In}_{13.4}$ (at.%) with the 0-5wt.% of Mo addition alloys denoted respectively as Mo0-Mo5 were presented in Fig. 1.

Depending on the molybdenum addition different types of the microstructures at room temperature were observed: (a) single phase martensite phase (Mo0), (b) parent + martensite + precipitates (Mo0.5-5). The SEM images show different contrast

corresponding to each phase. For the Mo0.5-Mo5 the lighter areas represent the untransformed martensite plates regions whereas the darker ones the parent phase. One can see that precipitates have submicron dimensions. The amount of the precipitates increases with the Mo addition. In Mo0 no precipitates have been stated whereas in Mo0.5 only a small amount of precipitates inside grains were present (Fig. 1 – Mo0.5 indicated by the green arrow). The intragrain precipitates are located randomly inside the matrix (parent or/and martensitic). Starting from the Mo1 alloy the precipitates (apart from the intragranular ones) join with each other creating “plait” like microstructure decorating the grain boundaries (Fig. 1 – green arrows in the Mo1). For each alloy (Mo0-Mo5) the very coarse matrix grains microstructure of 300 μm to even 2 mm in size were observed.

EDXS measurements of the received alloys revealed that the average chemical composition is in good agreement with the nominal one. In order to determine the distribution of the elements in precipitates, the EDXS SEM elemental mapping was recorded. The results for the Mo0.5 alloy are shown in Fig. 2.

One can see that the precipitates are enriched with Mo and Co in comparison to the matrix. The precipitates are very poor in In and consist less of Ni and Mn than the matrix.

Due to the small dimensions of the precipitates and relatively big interaction volume (bigger than precipitate size) we were not able to determine the exact chemical composition by the EDXS in the SEM. So the chemical composition of the precipitates was measured by the TEM EDXS for which the interaction volume is much smaller than the precipitates due to

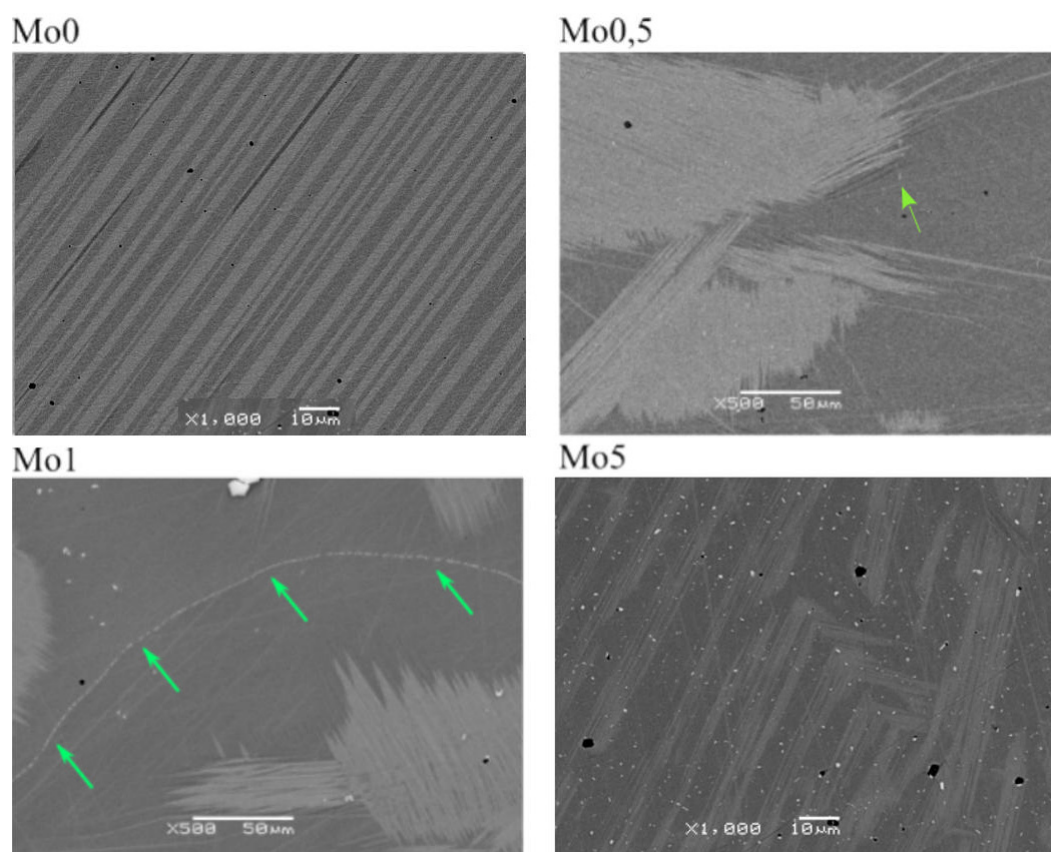


Fig. 1. SEM microstructure of the Mo0-Mo5 alloys

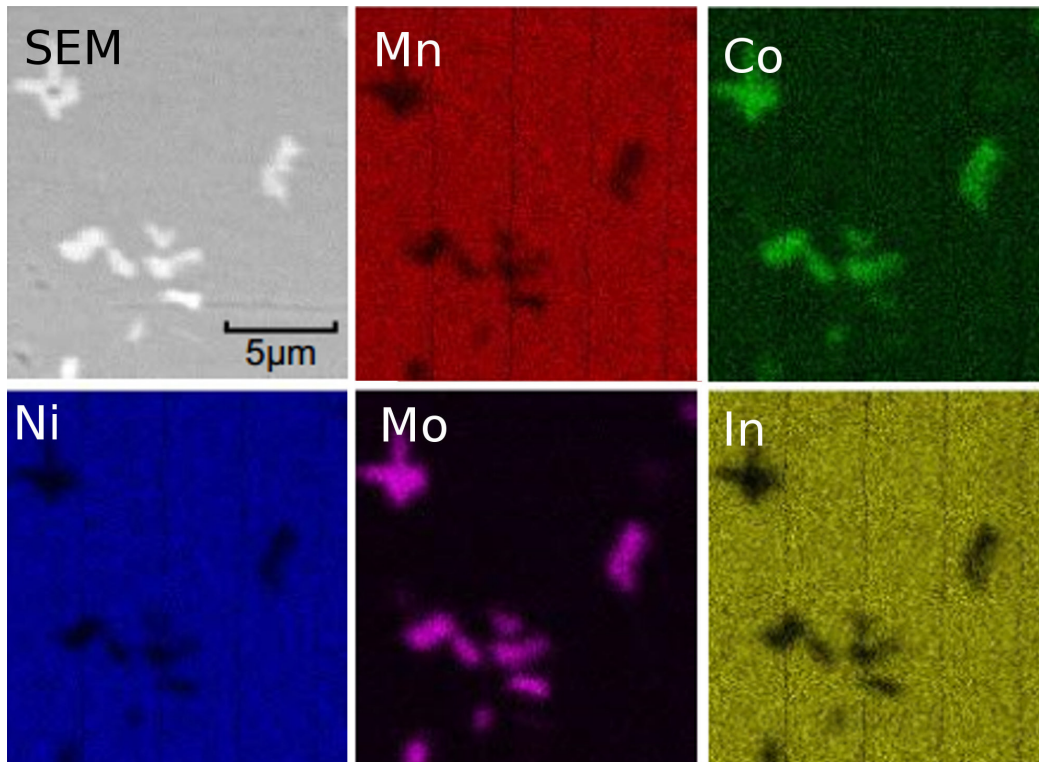


Fig. 2. EDXS elemental maps of Mo0.5 alloy

thin foil electron transparency. It was determined that Mo creates with Ni, Co, Mn solid solution. The average chemical composition of the precipitates of two investigated alloys is 17.4%Ni-36.2%Co-11.7%Mn-34.5%Mo (± 3 at.%). All molybdenum was located in the precipitates. EDX-TEM measurement revealed there were hardly any Mo in the matrix (below 0.5 at%).

Structure of the precipitates and matrix of the $\text{Ni}_{45.5}\text{Co}_{4.5}\text{Mn}_{36.6}\text{In}_{13.4}$ (at.%) alloys with the 0-5wt.% (0, 0.5, 1, 2, 5 wt.%) of molybdenum addition was determined by EBSD and TEM techniques. In Fig. 3 TEM results are presented. For all studied alloys at room temperature matrix of $\text{L2}_1/\text{B2}$ ordered phase with cubic (space group $\text{Fm}\bar{3}\text{m}$) and lattice parameters $a_0 = 5.98 \text{ \AA}$ was observed [9]. The $\{200\}$ and $\{111\}$ type superlattice reflections characteristic for B2 and L2_1 ordering in the Selected Area Diffraction Pattern (SAED) taken along $[110]$ zone axis were clearly seen (Fig. 3d).

The Dark Field (DF) TEM image obtained by $\{111\}$ superlattice reflection revealed the Anti Phase Domains (APD) which separates the highly ordered neighbouring regions with the same arrangement of atoms in the cell but shifted to each other by a fraction of lattice translation vector. The size distribution of the APD in the Mo0-Mo5 alloys are not uniform. The APD size for each studied alloys varies from 50 nm to about 500 nm. At room temperature in the $\text{Ni}_{45.5}\text{Co}_{4.5}\text{Mn}_{36.6}\text{In}_{13.4}$ (Mo0) martensite plates has been determined as modulated 7M monoclinic seven-layered structure (denoted also as 14M) with lattice parameter $a_0 = 4.23 \text{ \AA}$, $b = 5.62 \text{ \AA}$, $c_0 = 21 \text{ \AA}$, $\alpha = 90^\circ$, $\beta = 89.9^\circ$. Additionally in the Mo0.5-Mo5 alloys where precipitation process occurred the mixture of modulated and tetragonal L1_0 ($P 4_2/m$, $a_0 = b_0 = 7.81 \text{ \AA}$, $c_0 = 6.44 \text{ \AA}$) martensites structures has been

observed (Fig. 3b,e). The structure of precipitates in the Mo0.5-Mo5 alloys was identified as rhombohedral symmetry phase $\text{R}\bar{3}\text{m}$ with the lattice parameters $a_0 = b_0 = 7.76 \text{ \AA}$, $c_0 = 2.56 \text{ \AA}$, $\alpha = \beta = 90^\circ$, $\gamma = 120^\circ$ (Fig. 3f). The precipitates located mainly on the grain boundaries are surrounded by high dislocation density regions. TEM image (Fig. 3e) shows regular dislocation networks. The network contains usually screw dislocations. This sets of screw dislocations split into partial dislocations interacting with each other to form a network of partial dislocations bounding constricted and extended stacking faults. This dislocation is often called interface dislocation network and is observed in many alloys systems [19,20].

To determine the mechanical properties of the alloys the compression test was performed. Results of the tests are depicted in Fig. 4 and Tab. 1.

TABLE 1
The maximum compressive stress (R_c) and strain (ϵ_c)
for Mo0.5-Mo5 alloys

Alloy	R_c [MPa]	ϵ_c [%]
Mo0.5	558	24.4
Mo1	230	10.8
Mo2	188	5.5
Mo5	101	4.0

Mechanical properties decrease when the molybdenum content increase. The maximum compressive stress (R_c) decreases about 5 times from 558 MPa for 0.5 wt.% Mo addition to 101 MPa for 5 wt.% of Mo. Simultaneously the ductility of the al-

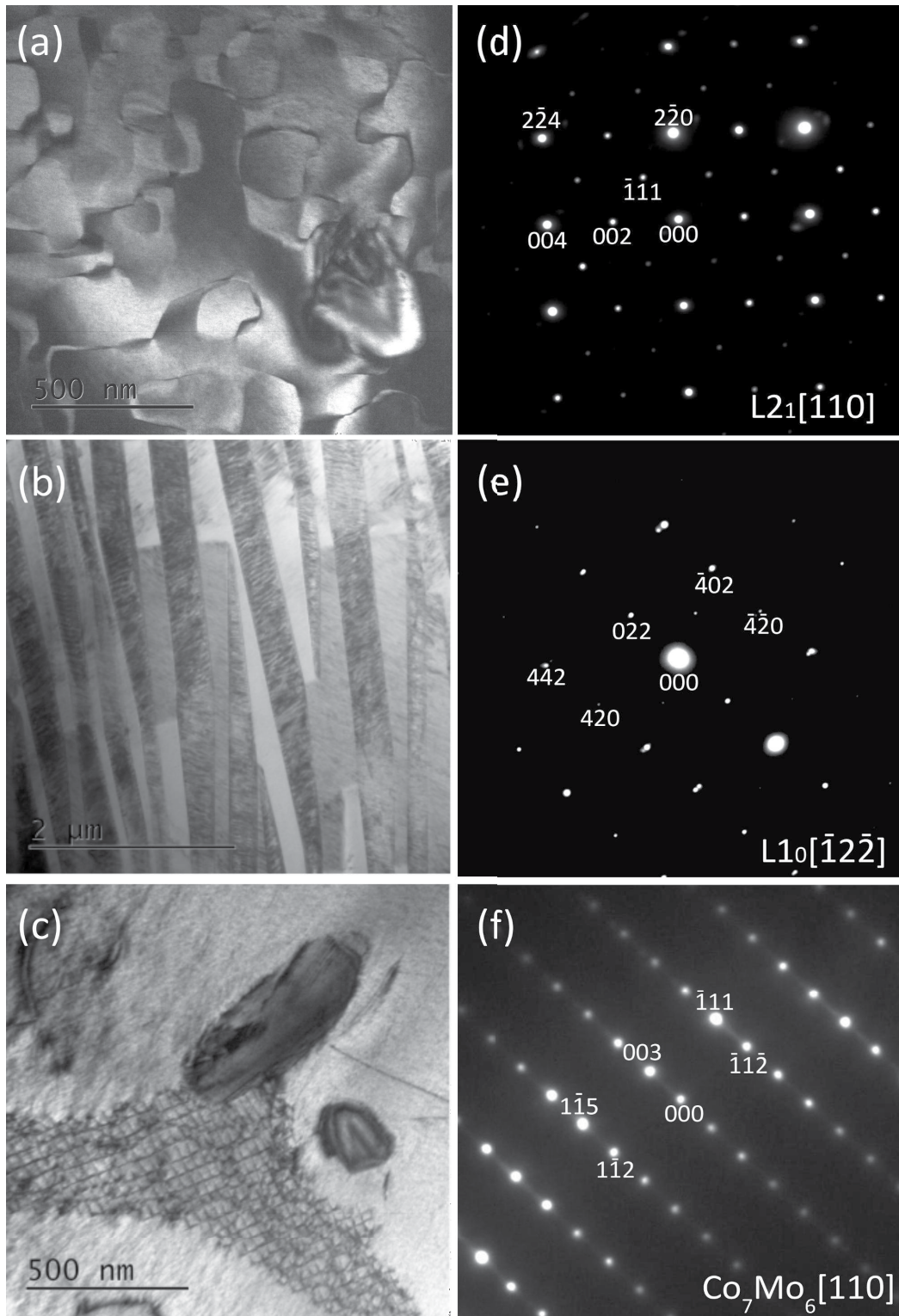


Fig. 3. DF (Dark Field) / BF (Bright Field) TEM images and SAED of parent phase (a,d), martensite phase (b,e) and precipitate (c,f) of Mo1 and Mo5 alloys

loys decreases with the molybdenum addition. The maximum compressive strain (ϵ_c) lowers more than 6 times from 24.4% to 4.0 % for Mo0.5 and Mo5 respectively. The presence of the Mo-rich precipitates located on the grain boundaries increases the brittleness of the alloys. In Fig. 5 the one can see mainly the intergranular fracture which by definition take place along the grain boundary of a material.

Many straight edges of the grain were noticed. The coarse grain matrix decomposition is clearly seen. The more Mo addition the more the cleavage fracture crack propagations are present in the sample. Additionally, many self-accommodating martensite variants can be noticed. Taking the above into account, the molybdenum addition promotes the nucleation process increasing the brittleness of the alloys.

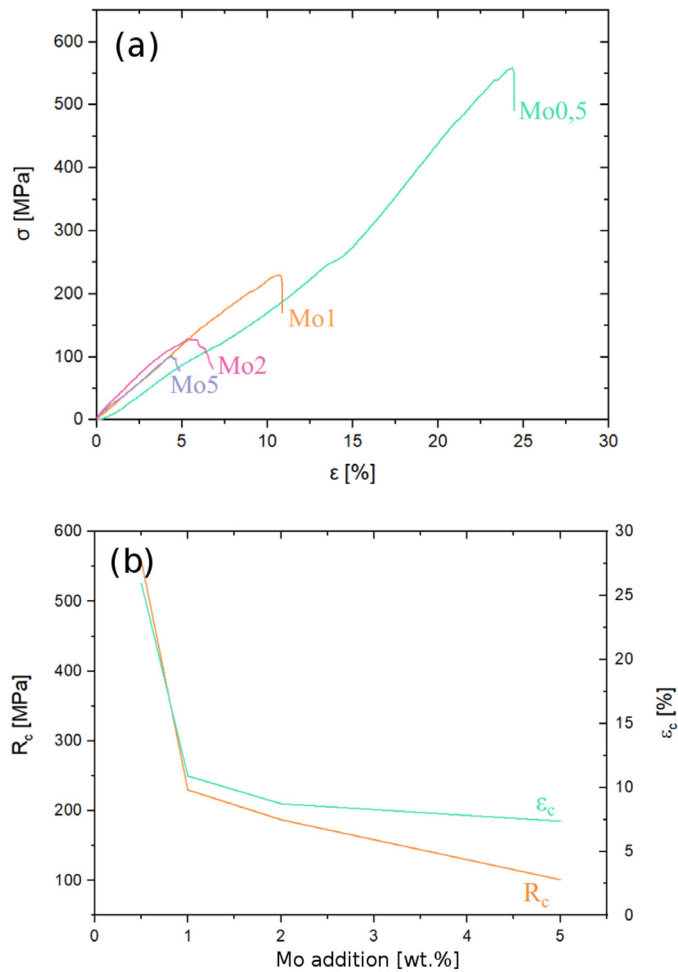


Fig. 4. Compression test results of the Mo0.5-Mo5 alloys: strain-stress curves (a), maximum compressive stress (R_c) and strain (ϵ_c) as a function of Mo addition

4. Summary

In this work, the influence of Mo addition on the structure and mechanical properties of the NiCoMnIn MSMA alloys have been studied. Series of $\text{Ni}_{45.5}\text{Co}_{4.5}\text{Mn}_{36.6}\text{In}_{13.4}$ (at.%) with the 0-5wt.% (0, 0.5, 1, 2, 5 wt.%) of molybdenum addition was prepared by the arc melting technique. All the alloys showed coarse grains the microstructure of the matrix of 0.5 mm to a few mm in size. Molybdenum addition affects the structure of the studied alloys. For all specimen containing Mo the precipitation process occurred. Mo-rich precipitates of the rhombohedral structure were located inside the grains as well as on the grain boundaries. The numbers of precipitates increase with the Mo content. Additionally, very fine regular sets of dislocation networks around precipitates were observed. For all the studied alloys the B2/L21 ordered structure of the parent phase were determined. The parent phase antiphase boundary domains of a 50-500 nm have been observed. Additionally, for the Mo-doped alloys, the mixture of modulated layered and tetragonal martensite plates was observed. The molybdenum addition strongly influenced the mechanical properties of the alloys. Unlike e.g. for the Ni-Mn-Sb [21] and Co-No-Ga [22] for which by the appropriate doping or thermal

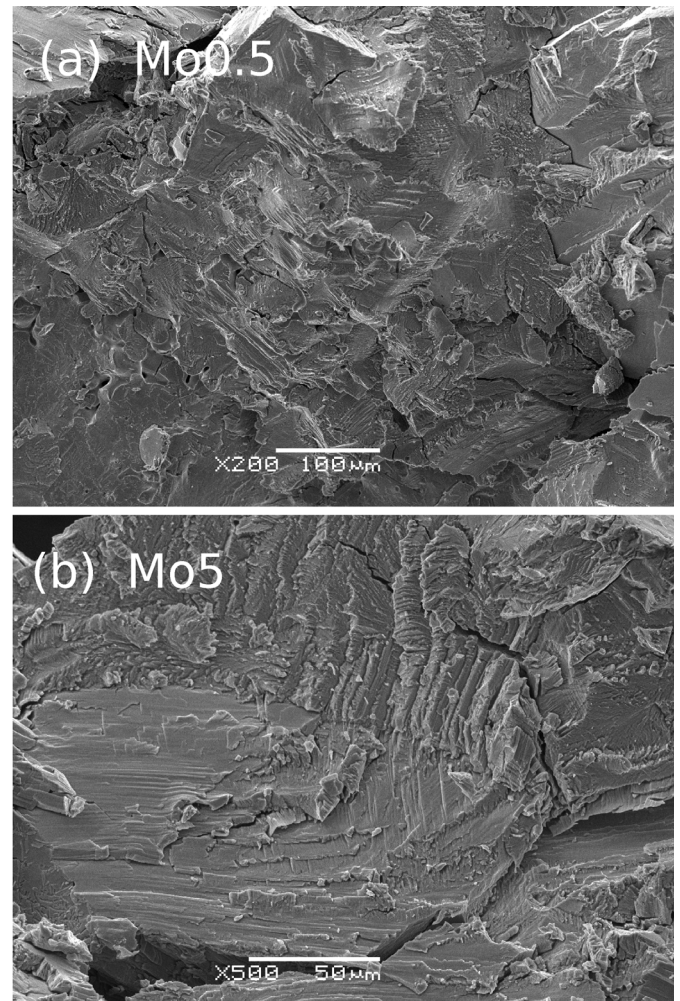


Fig. 5. SEM image of the fracture of Mo0.5 (a) and Mo5 (b) alloys after compression test

treatment on the grain boundaries the gamma phase precipitation process occurs (what significantly improves the ductility of the alloys) in the case of Mo-doped Ni-Co-Mn-In alloy precipitates play the opposite role. The presence on the grain boundaries of Ni-Co-Mn-In alloy the Mo-rich hard uncoherent precipitates led to the lack of the grain cohesion which increases the brittleness of the alloys. So the higher Mo content (means the more precipitates on the grain boundaries) as a consequence gives the more brittle alloys. Intergranular and cleaved fractures were observed. The maximum compressive stress (R_c) and strain (ϵ_c) decrease respectively 5 and 6 times (R_c from 558 MPa to 101 MPa for 5 and ϵ_c from 24.4 % to 4.0 %). The molybdenum addition to NiCoMnIn alloys promotes the precipitation process which increases the brittleness of the alloys.

REFERENCES

- [1] K. Ullakko et. al., Mater. J. Mater. Engin. Perform. **5**, 405-409 (1996), doi:10.1007/BF02649344.
- [2] A. Sozinov, A.A. Likhachev, N. Lanska, K. Ullakko, Appl. Phys. Lett. **80**, 1746-1748 (2002), doi: 10.1063/1.1458075.

- [3] R. Kainuma, Y. Imano, W. Ito, Y. Sutou, Magnetic-field-induced shape recovery by reverse phase transformation, *Nature* **439**, 957-960 (2006), doi:10.1038/nature04493.
- [4] H. Morawiec, T. Goryczka, A. Drdzeń, J. Lelątko, K. Prusik, Texture analysis of hot rolled Ni-Mn-Ga alloys, *Solid State Phenomena* **154**, 133-138 (2009)
- [5] K. Prusik, K. Bąldys, D. Stróż, T. Goryczka, J. Lelątko, Hot Extrusion of Ni-Based Polycrystalline Ferromagnetic Shape Memory Alloys, *Solid State Phenomena* **203-204**, 306-309 (2013), doi:10.4028/www.scientific.net/SSP.203-204.306.
- [6] S. Tamirisakandala, R.B. Bhat, J.S. Tiley, D.B. Miracle, Grain refinement of cast titanium alloys via trace boron addition, *Scr. Mater.* **53**, 1421-1426 (2005).
- [7] M. Ramudu, A. Satish Kumar, V. Seshubai, Influence of boron addition on the microstructure, structural and magnetic properties of Ni_{53.5}Mn_{26.0}Ga_{20.5} alloy, *Intermetallics* **28**, 51-57 (2012), doi:10.1016/j.intermet.2012.03.060.
- [8] S.N. Ghali, H.S. El-Faramawy, M.M. Eissa, J. Miner. Mater. Character. Engin., Influence of Boron Additions on Mechanical Properties of Carbon Steel **11**, 995-999 (2012).
- [9] K. Prusik, E. Matyja, M. Kubisztal, M. Zubko, R. Swadźba, Magnetic Properties and Structure of the Ni-Co-Mn-In Alloys with the Boron Addition, *Acta Physica Polonica* **131**, 1240-1243 (2017).
- [10] T. Krenke, E. Duman, M. Acet, X. Moya, L. Manosa, A. Planes, Effect of Co and Fe ~ on the inverse magnetocaloric properties of Ni-Mn-Sn, *J. Appl. Phys.* **102**, 033903 (2007).
- [11] C. Jing, Z. Li, H.L. Zhang, J.P. Chen, Y.F. Qiao, S.X. Cao, J.C. Zhang, Martensitic transition and inverse magnetocaloric effect in Co doping NiMnSn Heulser alloy, *Eur. Phys. J. B* **67**, 193-196 (2009).
- [12] B. Emre, N.M. Bruno, S. Yuce Emre, I. Karaman, Effect of niobium addition on the martensitic transformation and magnetocaloric effect in low hysteresis NiCoMnSn magnetic shape memory alloys, *Appl. Phys. Lett.* **105**, 231910 (2014).
- [13] X. Ding, X. Li, H. Huang, W. Matthias, S. Huang, Q. Feng, Effect of Mo addition on as-cast microstructures and properties of grey cast irons, *Materials Science & Engineering A* **718**, 483-491 (2018).
- [14] Q. Wu, C. Yang, F. Xue, Y. Sun, Effect of Mo addition on the microstructure and wear resistance of in situ TiC/Al composite Materials and Design **32**, 4999-5003 (2011).
- [15] Y. Chen, H.C. Jiang, S.W. Liu, L.J. Rong, X.Q. Zhao, The effect of Mo additions to high damping Ti-Ni-Nb shape memory alloys, *Materials Science and Engineering A* **512**, 26-31 (2009).
- [16] Y Al-Zain, H.Y. Kim, T. Koyano, H. Hosoda, T.H. Nam, S. Miyazaki, Anomalous temperature dependence of the superelastic behavior of Ti-Nb-Mo alloys, *Acta Materialia* **59**, (4) 1464-1473 (2011).
- [17] T. Maeshima, S. Ushimaru, K. Yamauchi, M. Nishida, M. Nishida, Effects of Sn Content and Aging Conditions on Superelasticity in Biomedical Ti-Mo-Sn Alloys, *Journal of the Japan Institute of Metals* **47** (3), 513-517 (2006).
- [18] H.Y. Kim, Y. Ohmatsu, J.I. Kim, H. Hosoda, S. Miyazaki, Mechanical Properties and Shape Memory Behavior of Ti-Mo-Ga Alloys, *Materials Transactions* **45**, 4, 1090-1095 (2004).
- [19] Y. Ru, S. Li, J. Zhou, Y. Pei, H. Wang, S. Gong, H. Xu, Dislocation network with pair coupling structure in {111} γ/γ' interface of Ni-based single crystal superalloy, *Scientific Reports* **6**, 2994, 1, 1-9 (2016), DOI: 10.1038/srep29941.
- [20] T. Akatsu, R. Scholz, U. Gosele, Dislocation structure in low-angle interfaces between bonded Si (001) wafers, *Journal of Materials Science* **39**, 3031-3039 (2004).
- [21] X. Tian, K. Zhang, C. Tan, E. Guo, Influence of Doping Tb on the Mechanical Properties and Martensitic Transformation of Ni-Mn-Sn Magnetic Shape Memory Alloys, *Crystals* **8**, 247, 1-11 (2018), doi:10.3390/cryst8060247.
- [22] K. Prusik, B. Kostrubiec, T. Goryczka, G. Dercz, P. Ochcin, H. Morawiec, *Materials Science and Engineering A* **481-482**, 330-333 (2008).